Sensors and Materials, Vol. 37, No. 1 (2025) 281–294
MYU Tokyo

S & M 3907

A Stable Imaging Platform of Low-altitude Unmanned Airship Remote Sensing System

Fengzhu Liu,[1] Mingliang Cao,[1] Ying Yang,[2*] and Yali Zhao[1]

[1]Beijing Institute of Surveying and Mapping, Beijing 100038, China
[2]National Geomatics Center of China, Beijing 100830, China

(Received August 9, 2024; accepted January 14, 2025)

Keywords: unmanned airship, three-axis stable platform, PID control, low-altitude aerial photography, aerial photogrammetry system

In this article, a three-axis stable platform control method based on a lightweight, low-precision global navigation satellite system (GNSS), inertial measurement unit (IMU) system, and proportion integration and differentiation (PID) algorithm is proposed to solve the stable imaging issues of a low-altitude unmanned airship aerial remote sensing system. The system utilizes a lightweight GNSS/IMU, which work with a dual global positioning system (GPS), connecting the camera system and flight platform through a three-axis stabilization platform, employing a PID control method with an open-loop control approach, and implementing stabilization control using a system-on-chip microcontroller for 32-bit (STM32) control chip circuit to address the camera attitude stabilization issue in the unmanned airship remote sensing system. The stability of the system is verified by a flight test, and the experimental results also show that the method can effectively isolate the effect of the instability of the unmanned airship attitude on the imaging system and effectively improve the imaging quality, which is of considerable significance for improving the accuracy of the unmanned airship aerial survey system.

1. Introduction

As a flexible aerial photography platform, an unmanned aerial survey system has been widely used in various aspects of national economy and construction, such as agriculture, water conservation, military, geophysical exploration, surveying and mapping, and disaster relief.(1,2) Unmanned airships have many advantages(3) as a flying platform that can carry out large-scale surveying and mapping tasks over cities. First, their flight speed can be very low, which can effectively reduce the image motion problem caused by high-speed movement and improve image clarity. Second, the load capacity of unmanned flights can be very high, and 10–70 kg of equipment can be carried. The flight time of unmanned airships is also relatively long, reaching 3–5 or even longer. Unmanned airships also have their own shortcomings. The most prominent problem is that the platform has poor flight stability and is more susceptible to airflow, which

*Corresponding author: e-mail: yangying@ngcc.cn
https://doi.org/10.18494/SAM5300

ISSN 0914-4935

directly affects the quality of camera data acquisition and the difficulty and accuracy of subsequent data production.[4–7]

The disturbance of the flight platform is an important factor affecting the imaging quality of the optical imaging system, especially for the photogrammetric camera system. The camera imaging mode and image posture have a direct impact on the quality of image acquisition and the accuracy of subsequent data processing.[8–10] The disturbance of the flight platform can be divided into two parts: high frequency and low frequency. The high frequency can generally be achieved by a shock-absorbing device (such as a shock-absorbing gasket).[11–14] The causes of low-frequency vibration are more complicated, such as the stability of flight control system, the change of weather conditions during flight, and other reasons. On traditional aerial photography platforms, the stable platform can well isolate the interference of the flight platform disturbance to the camera system, ensure the smooth operation of the imaging system, and thus ensure the reliability of the camera system and data quality.[15–18] Traditional stable platforms such as Germany SSM150, Switzerland PAV30, and other international brand stable platforms generally weigh 15-50 kilograms and need to be equipped with high-precision position and orientation systems (POSs), such as high-precision fiber optic gyroscopes. The power consumption is also more than 100 watts and is expensive. In terms of the control angle range, the pitch and roll can generally only reach about 10°. These characteristics limit its application in unmanned aerial vehicles. It is very urgent to develop a lightweight and small stable platform that can be used for low-altitude aerial photography platforms. In combination with the characteristics of unmanned airships and the feasibility of equipment installation, we propose a low-precision, lightweight, and small dual global positioning system (GPS)-assisted global navigation satellite system (GNSS)/inertial measurement unit (IMU) combined inertial navigation system. We adopted an installation method that is different from the existing attitude survey system and camera system rigid connection, and installed the camera and GNSS/IMU system in isolation. Combined with the digital proportion integration and differentiation (PID) control algorithm, the light and small three-axis stable platform is controlled by the system-on-chip microcontroller for 32-bit (STM32) control chip to achieve the three-axis stable imaging of the camera system of the unmanned airship platform.

2. Light and Small Three-axis Stable Platform Control System Structure

2.1 Stable platform and control method of traditional aerial survey system

Traditional aerial camera stabilization platforms, such as Leica PAV30, PAV80, and PAV100, are mostly specially designed for aerial manned aircraft platforms and are used for large aerial cameras, such as RC30, DMC, UCD, and other large-area array cameras. These types of stable platforms need to be equipped with a high-precision GNSS/IMU combined inertial attitude survey system to work (Canada POS AV 510 has dynamic accuracies of 0.005° for pitch and roll angles and 0.03° for heading angles). In the control mode, a binary control loop design is adopted, that is, the high-precision gyroscope attitude survey system is rigidly connected to the camera system at a fixed angle, and directly measures the real-time attitude of the camera

system. The signal is directly transmitted to the stable platform for control. The stable platform control instructions correct and compensate the camera attitude, and then correct the attitude survey system. The whole system forms a closed loop. The control goal of the stable platform is to ensure that the attitude of the camera system is around the target value, thus realizing stable imaging.

Traditional stable platforms are widely used for large aerial photography platforms and have achieved good results. The design size and equipment operation requirements make it difficult to apply them to low-altitude, lightweight, and miniaturized low-altitude platforms. Therefore, it is necessary to design the equipment to be lightweight and miniaturized and to reduce, for example, the power consumption, volume, and weight. of the equipment, so that it can meet the requirements of the airship platform. On the basis of a lightweight dual-GPS-assisted GNSS/IMU combined inertial navigation system, we adopted a digital PID control algorithm to realize a lightweight and small three-axis stable platform control method.[12,17] The low-precision attitude survey system is used on the unmanned airship platform to achieve the stable imaging of the aerial photography platform camera system, which is very meaningful for improving the quality of the aerial images of unmanned aerial photography platforms, post-photogrammetry data processing, and the geometric survey accuracy of images.

2.2 Lightweight three-axis stable platform system and control process

We conducted a stabilization platform research and development test for unmanned airship platforms. The airship platform system mainly includes a boat capsule, a power cabin, a direction control rudder, a flight control system, a camera mounting cabin, a three-axis stabilization platform, a combined wide-angle camera system, and dual GPS antennas. In terms of equipment installation, the dual GPS combined GNSS/IMU inertial navigation attitude survey system is installed in the camera mounting cabin at the front end of the airship to remain firmly connected to the airship. Dual GPS fillers are installed at both ends of the airship, and the baseline length meets the working requirements of the equipment and maintains a fixed connection with the GNSS/IMU inertial navigation attitude survey system. The three-axis stable platform and the mounting cabin are fixed and connected with special connection interfaces to maintain rigidity. The combined wide-angle camera module is mounted on the inner ring bracket of the three-axis stabilization platform for fixation.

The control system consists of the following equipment: the GNSS/IMU combined inertial navigation system assisted by the light and small dual GPS, the mechanical structure of the digital servo gear control of the stable platform, and the position sensitive detector (PSD) system based on the digital PID algorithm. The system control flow is shown in Fig. 1.

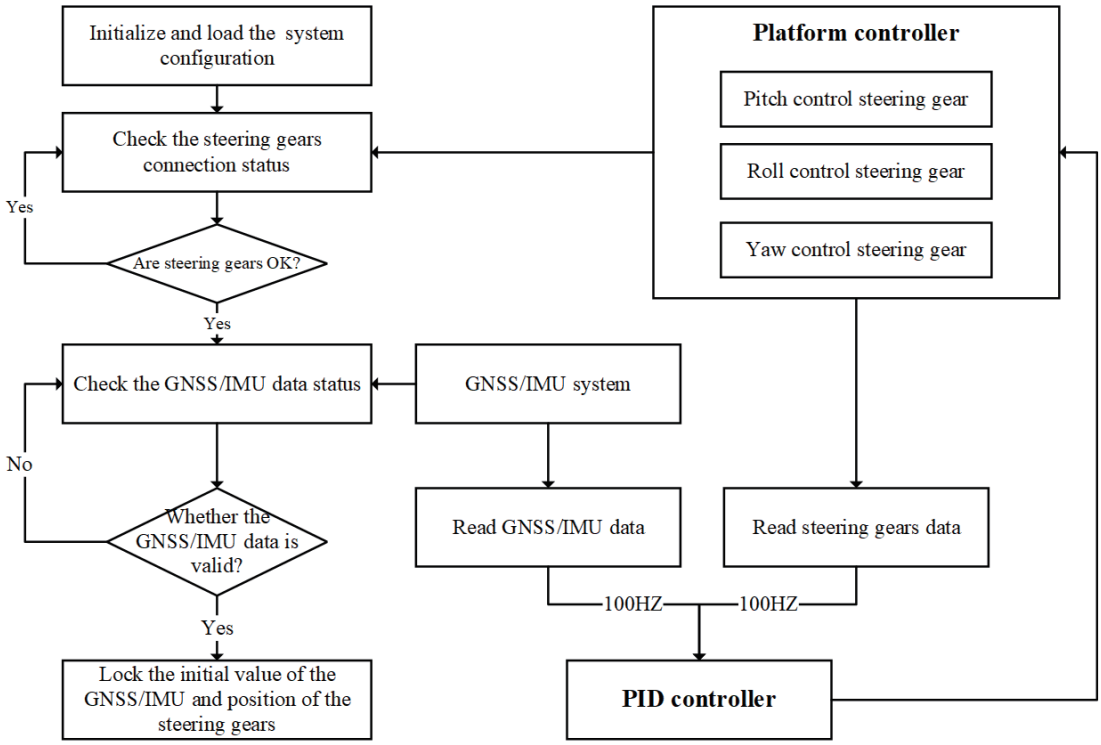

Fig. 1. Main workflow of lightweight three-axis stable platform.

3. Control Algorithm of Stable Platform

3.1 Technical characteristics of PID control algorithm

PID is a proportional, differential, and integral control algorithm. Proportional control is the simplest control mode, and the output of the controller is proportional to the input error signal. In integral control, the output of the controller is proportional to the integral of the input error signal. In differential control, the output of the controller is proportional to the differential of the input error signal. The automatic control system may oscillate or even lose stability in the adjustment process to overcome the error. The reason is that there are large inertia or lag components, which have the function of suppressing the error, and their changes always lag behind the changes of errors. Figure 2 shows a simple process of the PID control algorithm.

The continuous form of the PID algorithm is as follows:[14]

$$u(t) = K_p\left[e(t) + \frac{1}{T_i}\int_0^t e(t)\,d_t + T_d\frac{de(t)}{dt}\right], \tag{1}$$

where K_p is the proportionality constant, T_i is the integration constant, T_d is the differential constant, $e(t)$ is the input of the PID controller, and $u(t)$ is the output of the PID controller. Its discrete equation is

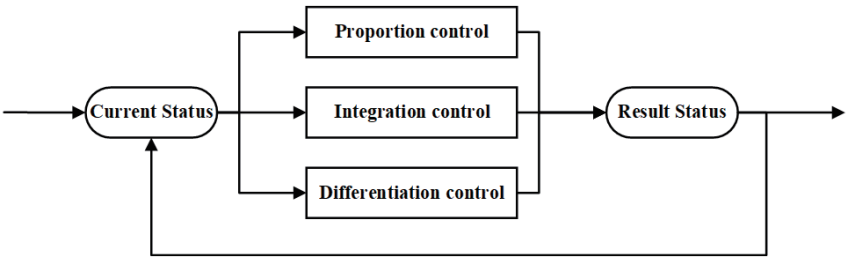

Fig. 2. PID algorithm flowchart.

$$u(k) = K_p * e(k) + K_i * \sum_{i=0}^{k} e(i) + K_d * \left(e(k) - e(k-1)\right), \tag{2}$$

where K_p is the proportionality constant, K_i is the differential constant, K_d is the integration constant, $e(k)$ is the controller input, and $u(k)$ is the controller output. The data of the attitude survey system always lags behind the real-time data. This feature of the PID control algorithm is used to improve the dynamic characteristics of the system during the adjustment process, ensure the stability of the servo control and the stability of the camera attitude, and avoid the instability and jitter of the system caused by high-frequency changes.

3.2 Structural design of light and small three-axis stable platform

Compared with traditional large aerial photography platforms, the attitude stability of airship platforms is worse and is considerably affected by airflow. The hanging axle design is adopted, which realizes a greater degree of freedom of angle control and meets the requirements of pitch angle −35–+35°, roll angle −35–+35°, and yaw angle −45–+45° of the unmanned airship aerial survey system. The stabilization platform includes three rotating control frames. The camera system is mounted on the inner ring control platform and connected to the central control ring through a digital steering gear. The central ring control shaft is connected to the outer ring through the digital steering gear in the vertical axis, and the external frame is rigidly connected to the platform pendant through the main shaft. Each rotating shaft can be controlled in parallel to improve the control efficiency. The platform is made of carbon fiber material, which not only meets the rigidity requirements of hardware, but also ensures that the weight of the platform will not affect the safety of the flight platform. The mechanical design drawing of the three-axis stable platform is shown in Fig. 3.

We define the angle of rotation about the *X*-axis as ω, the angle of rotary about the *Y*-axis as φ, and the angle of rotary about the *Z*-axis as κ. According to the rotary characteristics of the stable platform, the rotary matrix formed in three directions can be obtained as

$$T_{\omega\varphi\kappa} = T_\kappa * T_\varphi * T_\omega, \tag{3}$$

where

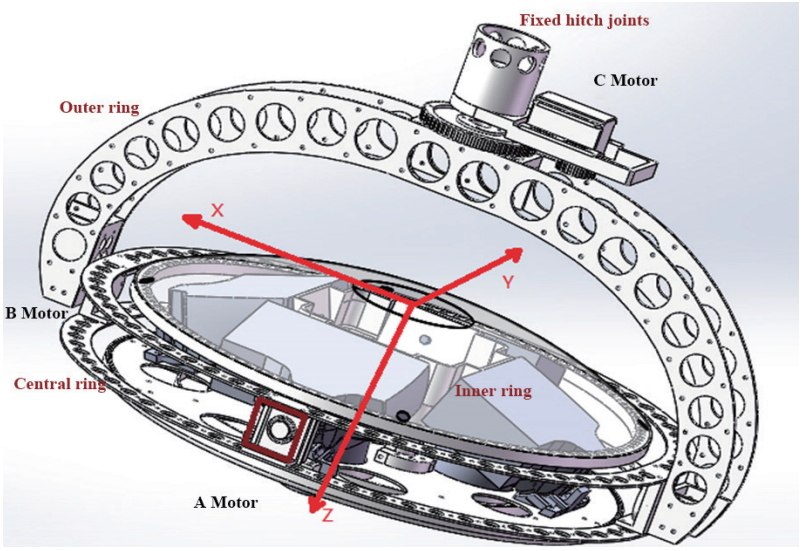

Fig. 3. (Color online) Mechanical drawing of three-axis stable platform design.

$$T_{\omega}=\begin{bmatrix}1,0,0\\0,\cos(\omega),\sin(\omega)\\0,-\sin(\omega),\cos(\omega)\end{bmatrix},$$
$$T_{\varphi}=\begin{bmatrix}\cos(\varphi),0,-\sin(\varphi)\\0,1,0\\\sin(\varphi),0,\cos(\varphi)\end{bmatrix}, \quad (4)$$
$$T_{\kappa}=\begin{bmatrix}\cos(\kappa),\sin(\kappa),0\\-\sin(\kappa),\cos(\kappa),0\\0,0,1\end{bmatrix}.$$

The control of the platform's three rotating axes is parallel, which enhances the platform's response speed. Additionally, to reduce electromagnetic interference between devices (such as motors), digital servos are used for rotational control, which can achieve precise rotation control within a range of 0 to 300 degrees corresponding to 1024 steps. The control precision is 0.3 degrees. Communication is accomplished using the RS485 serial digital communication method, ensuring that control commands are not affected by other electromagnetic sources, thus maintaining the normal operation of the control system and enhancing system stability.

3.3 Introduction of dual GPS light and small attitude survey instrument

The attitude survey system is the core component of the entire control system. We used the XW-GI5631 dual-GPS-assisted GNSS/IMU combined inertial navigation system independently

developed by China. The system consists of a GNSS/IMU combined navigation data solution system control board with two GPSs and a low-precision three-axis gyroscope. The dual GPS orientation combined with the gyroscope solution improves the survey accuracy of the system, especially the accuracy of the yaw angle. The yaw angle survey accuracy is 0.2° and the attitude angle is 1.0°. The three angles *Pitch*, *Roll*, and *Head* of the combined inertial navigation output correspond to the pitch, roll, and head angles, respectively, and their definitions are shown in Fig. 4.

The angles of attitude survey, *Pitch*, *Roll*, and *Head*, are three relatively independent rotation angles, which are different from the angle characteristics of the stable platform above. The rotation matrix is

$$\boldsymbol{R} = R_{roll} * R_{pitch} * R_{head}, \tag{5}$$

where

$$\begin{aligned} R_{head} &= \begin{bmatrix} \cos(head), \sin(head), 0 \\ -\sin(head), \cos(head), 0 \\ 0, 0, 1 \end{bmatrix}, \\ R_{pitch} &= \begin{bmatrix} \cos(pitch), 0, -\sin(pitch) \\ 0, 1, 0 \\ \sin(pitch), 0, \cos(pitch) \end{bmatrix}, \\ R_{roll} &= \begin{bmatrix} 1, 0, 0 \\ 0, \cos(roll), \sin(roll) \\ 0, -\sin(roll), \cos(roll) \end{bmatrix}. \end{aligned} \tag{6}$$

The device has two GPS antennas, designated as the front and rear antennas, which must be installed at the front and rear ends in the direction of flight, with a distance requirement of more than 2 m, and they must maintain a relatively fixed relationship with the IMU device. Therefore, they cannot be fixed above the camera as in traditional single GPS integrated inertial navigation systems, which would ensure a rigid connection with the camera, nor can they be controlled

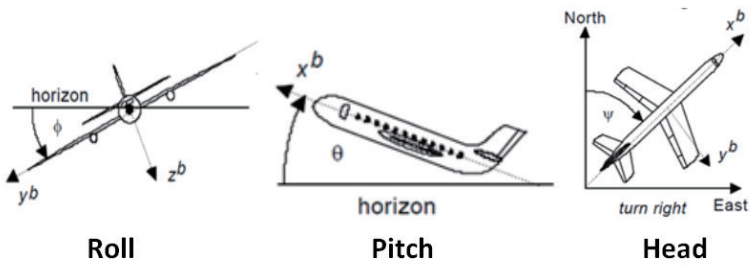

Fig. 4. Definitions of three-axis survey angles of GNSS/IMU system.

using traditional closed-loop control methods. This is a key issue addressed by the method proposed in this paper.

3.4 Control method of light and small three-axis stable platform

The control goal of the stable platform is to combine the inertial navigation attitude system to measure the real-time attitude data of the airship and send it to the control circuit of the stable platform. The control chip calculates the attitude of the airship and the current state of the three-axis steering gear of the stable platform, calculates the rotary of the steering gear, and combines the PID control system to control the rotary, so as to offset or reduce the effect of the airship swing on the camera, keep the camera consistent with the designed route, and take photographs vertically downward.

According to the structure of the stable platform, the coordinate system relationship between the attitude survey system of the stable platform and the camera system is established. When the system is initialized, the camera platform and the combined inertial attitude survey system are installed consistently. The inertial navigation data recorded during initialization is ($roll_0$, $pitch_0$, $head_0$). $head_0$ is the flight belt angle configured by the flight route. The neutral position of the initialized digital steering gear is recorded as (Pa_0, Pb_0, Pc_0), and the constant of steering gear calibration and angle conversion is γ.

We set a point in the camera coordinate system as $P(U, V, W)$. In the initial state, the point in the coordinate system $O–XYZ$ and $O–UVW$ is consistent. When the flight attitude changes, the attitude survey system survey data changes. The angle measured by the attitude meter at the moment t is recorded as ($roll_t$, $pitch_t$, $head_t$). Assuming that the servo does not rotate, the stabilizing and camera platforms rotate together with the attitude indicator. The new coordinates of P are $P(U', V', W')$. If the servo of the stable platform is controlled to rotate, the coordinates of point P are restored to $P(U, V, W)$. The goal of restabilizing the camera platform is then achieved, and the sighting axis returns to its vertical downward position.

Combined with the rotary characteristics of the attitude indicator and the stable platform control system, we make the transformation matrix in the middle of the transformation of the attitude meter from the state ($roll_0$, $pitch_0$, $head_0$) to ($roll_t$, $pitch_t$, $head_t$) be R'; then, there is

$$R_t = R' * R_0, \tag{7}$$

where

$$\begin{aligned} R_0 &= R_{roll_0} * R_{pitch_0} * R_{head_0}, \\ R_t &= R_{roll_t} * R_{pitch_t} * R_{head_t}. \end{aligned} \tag{8}$$

Then, the transformation equation of $P(U, V, W)$ to $P(U', V', W')$ is

$$\begin{bmatrix} U' \\ V' \\ W' \end{bmatrix} = R' * \begin{bmatrix} U \\ V \\ W \end{bmatrix}. \tag{9}$$

The process of inverse transformation can be solved according to the change of the attitude meter, and the inverse transformation matrix is the inverse matrix T_k of R'; then, we can obtain

$$T_k = (R_t * R_0)^T. \tag{10}$$

According to the rotary characteristics of the stable platform, namely,

$$T_k = T_\kappa * T_\varphi * T_\omega, \tag{11}$$

we solve and obtain the rotary angle of the three axes as [initialize and define the neutral position (ω, φ, κ) angle (0, 0, 0)]

$$\begin{aligned} \varphi &= a\sin\left(-T_k(7)\right), \\ \omega &= a\tan 2\left(T_k(8), T_k(9)\right), \\ \kappa &= a\tan 2\left(T_k(4), T_k(1)\right). \end{aligned} \tag{12}$$

The target scales of the three servos are converted to (Pa_t, Pb_t, Pc_t)

$$\begin{aligned} Pa_k &= Pa_0 + \omega * \gamma, \\ Pb_k &= Pb_0 + \varphi * \gamma, \\ Pc_k &= Pc_0 + \kappa * \gamma. \end{aligned} \tag{13}$$

We read the real-time state position scale of the three steering gears as (Pa_t, Pb_t, Pc_t); then, the target position $P_t'(k)$ of PID control of the steering gear at time t is

$$P_t'(k) = K_p * e(k) + K_i * \sum_{i=0}^{k} e(i) + K_d * \left(e(k) - e(k-1)\right) + P_0, \tag{14}$$

where $e(k) = (P_k - P_t)$, P_0 is the scale value of the initial horizontal position of the steering gear, which can be used to obtain the target positions of the three steering gears ($Pa_t'(k)$, $Pb_t'(k)$, and $Pc_t'(k)$) and then control the steering gear to achieve the control goal of stabilizing the platform. The parameters of PID control are related to the working characteristics of the flight platform. The three axes are different. The parameters are obtained through ground debugging and flight tests.

4. Experiment and Results

4.1 Introduction to survey platform

The test flight and camera system are both an unmanned airship aerial survey platform and a light, small, and extra-wide angle combined four-piece camera system independently developed by China. The flight area is about 10 km^2, the flight altitude is 250 m, and the ground resolution of the images is about 5 cm. Two sorties were flown and a total of 1969 images were obtained. The route is planned to be north–south, that is, the route angle is 0°, the wind force on site is level 3, the airship's flight state is basically normal, and there is a "nodding", that is, there is a periodic slow decline in altitude and then a climb during the flight.

4.2 Results and discussion

The comparative test method is used to conduct two independent flight tests on the same platform, the same camera, and similar weather conditions with and without a stable platform. In the data analysis, we used the external orientation elements of "aerial triangulation" encryption orientation to analyze the working state of the stable platform, and the three axes are independently analyzed and compared. Figures 5–7 show the attitude data without a stable platform.

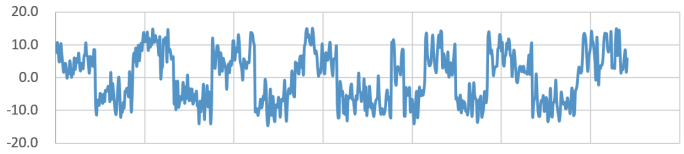

Fig. 5. (Color online) Pitch angle deviation curve.

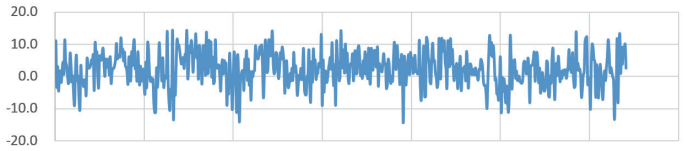

Fig. 6. (Color online) Rolling off the curve.

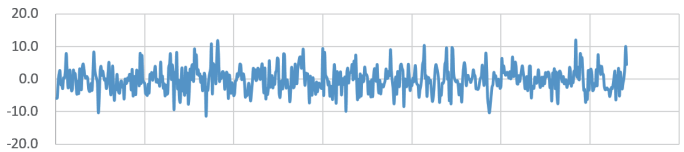

Fig. 7. (Color online) Yaw angle deviation curve.

The experimental results show that when there is no stable platform, the flight attitude of the airship has a significant impact on the operation of the camera because of the rigid connection between the camera system and the airship system. The data in Table 1 shows that owing to the effect of the airship platform, the three angle changes of pitch, roll, and yaw are mainly distributed around 10°. Among them, the pitch angle is very regularly affected by the attitude of the airship, which is very consistent with the attitude characteristics of the airship platform flying upwind and downwind (the wind direction at the flight site is consistent with the flight direction). Figures 8–10 show the data deviation distribution of the experimental results with a stable platform.

The experimental results in Table 2 show that the deviation range of angular elements of all images (the deviation of yaw angle is determined as the deviation from the designed route angle) is less than 3°, and more than 95% of the deviation errors of three axial control angles are less than 2° and more than 60% are distributed within 1°, especially 65% of the yaw angle errors are

Table 1
Statistics of attitude angles of flight tests without stable platform.

Limit	Pitch Angle (%)	Roll Angle (%)	Deflection Angle (%)
<15°	100.00	100.00	100.00
<10°	88.24	75.27	88.55
<3°	40.46	16.79	25.19
<1°	13.44	3.82	7.63

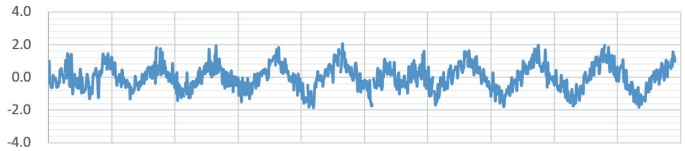

Fig. 8. (Color online) Pitch angle deviation curve.

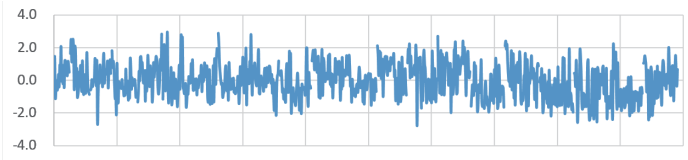

Fig. 9. (Color online) Rolling off the curve.

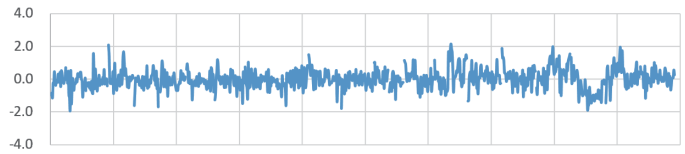

Fig. 10. (Color online) Yaw angle deviation curve.

Table 2
Stable platform control angle deviation distribution statistics.

Limit	Pitch Angle (%)	Roll Angle (%)	Deflection Angle (%)
<3°	100.0	100.0	100.0
<2°	99.59	95.67	99.79
<1°	80.08	62.02	89.47
<0.5°	46.64	33.23	67.29

distributed within 0.5°. The accuracy of yaw angle control is higher than those of roll and pitch angle control, which is consistent with the nominal accuracy of the POS system, and the effectiveness of control and the effect of POS accuracy on control accuracy are verified. In the experimental data, some samples are greater than 2°. The preliminary analysis may be related to the overshoot phenomenon of the stable platform and the steering of the flying platform. The steering process of the airship platform is relatively fast and the turning radius is relatively small, which may cause the angle to change too fast, and the steering gear speed cannot keep up. The overall analysis shows that the control ideas and methods proposed in this study have good experimental results, and the control accuracy has reached the research goal. It can well isolate the effect of airship platform flight swing on the imaging system and improve the image quality.

5. Conclusion

On the basis of the characteristics of the current unmanned airship aerial survey system and the difficulties in data acquisition, especially for the problems of the stabilization platform, we analyzed and introduced the existing aerial camera stabilization platform and put forward a light and small three-axis stabilization platform control method based on a dual GPS antenna inertial attitude survey system and PID control algorithm, which has the characteristics of small weight, low power consumption, low cost, large correction angle, and simple structure, and realizes the high-precision control of a three-axis stabilization platform with a low-precision POS system combined with the PID algorithm. Combined with the experimental results of the unmanned airship platform, we showed that this method can control the camera well for stable imaging, which is of considerable significance to improve the image quality, data processing accuracy, and mapping accuracy of the unmanned airship aerial survey system.

References

1 J. Jia, H. B. Ai, and L. Zhang: Bull. Surv. Mapp. **5** (2013) 62 (in Chinese). https://www.cqvip.com/doc/journal/953644942
2 J. Sun, Z. J. Lin, and H. X. Cui: Remote Sens. Inf. **26** (2003) 48 (in Chinese). https://doi.org/10.3969/j.issn.1000-3177.2003.01.014

3 X. D. Peng and Z. J. Lin: Sci. Surv. Mapp. **34** (2009) 11 (in Chinese). https://doi.org/10.1016/S1874-8651(10)60080-4
4 H. X. Cui: Research on Low altitude Digital Photogrammetry System for Drones (Wuhan University, Wuhan, 2006).
5 X. Y. Zong: Bull. Surv. Mapp. **2** (2011) 90 (in Chinese). https://www.cqvip.com/QK/93318X/20112/36768767.html
6 Y. Zhang: Wuhan Univ. Inf. Sci. Ed. **34** (2009) 284 (in Chinese). https://doi.org/10.1042/BSR20080061
7 Z. J. Lin, F. F. Xie, and G. Z. Su: Acta Geodaetica et Cartographica Sinica **43** (2014) 991 (in Chinese). https://doi.org/10.13485/j.cnki.11-2089.2014.0146
8 Z. Z. Wang: Photogrammetry (Wuhan University Press, Wuhan, 2007).
9 J. Q. Zhang, L. Pan, and S. G. Wang: Photogrammetry (Wuhan University Press, Wuhan, 2003).
10 J. L. Xu, T. Zhu, and H. W. Bian: J. Inst. Sci. **28** (2007) 914 (in Chinese). https://doi.org/10.3321/j.issn:0254-3087.2007.05.028
11 Y. Pu and Q. Li: J. CHN. Inertial Tech. **15** (2007) 171 (in Chinese). https://doi.org/10.3969/j.issn.1005-6734.2007.02.012
12 W. Ji and Q. Li: Acta Aeronautica et Astronautica Sinica **28** (2007) 191 (in Chinese). https://doi.org/10.3321/j.issn:1000-6893.2007.01.037
13 X. Y. Shen, H. L. Chen, and S. Liu: Electronics Optics & Control **18** (2011) 46 (in Chinese). https://doi.org/10.3969/j.issn.1671-637X.2011.04.012
14 J. M. Hilkert: IEEE Control Systems Magazine **28** (2008) 26. https://doi.org/10.1109/MCS.2007.910256
15 T. Zhu, N. D. Bao, J. N. Xu B, and W. W. Bian: Journal of Chinese Inertial Technology. **10** (2002) 42 (in Chinese). https://doi.org/10.3969/j.issn.1005-6734.2002.03.008
16 S. K. Yang, J. F. Wang, and J. Y. Wang: Electronics Optics & Control. **15** (2008) 62 (in Chinese). https://doi.org/10.3969/j.issn.1671-637X.2008.02.017
17 Z. Wang, Q. K. Li, F. D. Li, J. Tong, and Z. K. Wang: Optics & Optoelectronic Technology **11** (2013) 65. https://www.cqvip.com/doc/journal/948777205
18 M. K. Masten: IEEE Control Systems Magazine **28** (2008) 47. https://doi.org/10.1109/MCS.2007.910201

About the Authors

Fengzhu Liu received her Ph.D. degree from Wuhan University, China, in 2016. She is working at the Beijing Institute of Surveying and Mapping and is a researcher at the Beijing Key Laboratory of Urban Spatial Information Engineering, and since 2018, she has been a senior engineer. Her research interests are in urban 3D spatial data acquisition and processing. (540508818@qq.com)

Mingliang Cao received his B.S. degree from Beijing University of Civil Engineering and Architecture, China, in 2019. Since 2019, he has been working at the Beijing Institute of Surveying and Mapping as an assistant engineer. His research interests include real-world 3D model reconstruction, multi-source data fusion modeling, 3D scene optimization, and digital twin updating. (2622317678@qq.com)

Ying Yang received his B.S. degree from Wuhan University, China, in 2007, his M.S. degree from the Chinese Academy of Sciences, China, in 2010, and his Ph.D. degree from Wuhan University, China, in 2017. From 2010 to 2013, he was an assistant professor at Chinese Academy of Surveying and Mapping, China. Since 2017, he has been an engineer at National Basic Geomatics Center of China. His research interests are in photogrammetry, UAV systems, and sensors. (yangying@ngcc.cn)

Yali Zhao received her M.S. degree from Capital Normal University, China, in 2021. Since 2021, she has been working at the Beijing Institute of Surveying and Mapping as an assistant engineer. Her research interests are in geographic information science and land subsidence monitoring and analysis research based on interferometric synthetic aperture radar (InSAR). (18335156979@163.com)